ISSN 0023-1584, Kinetics and Catalysis, 2007, Vol. 48, No. 1, pp. 1–7. © MAIK "Nauka/Interperiodica" (Russia), 2007.
Original Russian Text © I.K. Larin, A.I. Spasskii, E.M. Trofimova, L.E. Turkin, 2007, published in Kinetika i Kataliz, 2007, Vol. 48, No. 1, pp. 5–11.

Mechanism and Kinetics of the Reaction between Hydrogen Iodide and Ozone

I. K. Larin, A. I. Spasskii, E. M. Trofimova, and L. E. Turkin

Institute of Energy Problems of Chemical Physics, Russian Academy of Sciences, Chernogolovka, Moscow oblast, 142432 Russia

e-mail: EMTrofimova@mtu-net.ru

Received April 19, 2005

Abstract—The reaction between hydrogen iodide and ozone at 295 K has been investigated by the resonance fluorescence method applied to the detection of iodine atoms. A chain mechanism is suggested for this reaction. The chain initiation rate constant is $k_1 = (5.45 \pm 1.80) \times 10^{-17}$ cm^3/s, and the chain propagation rate constant is $k_3 = (1.1 \pm 0.4) \times 10^{-12}$ cm^3/s.

DOI: 10.1134/S0023158407010016

The NaCl concentration in aerosols that are formed over the sea surface by water drops separating from waves is lower than the NaCl concentration in the seawater. Furthermore, in a given region, the ozone level is lower over the sea than over land. These facts were explained by sodium chloride reacting with various substances, including ozone, on the surface of aerosol droplets [1]. As a result, Cl^- is oxidized to Cl^0 and chlorine is released to the atmosphere. Later, it was demonstrated that sodium chloride is indeed oxidized on the surface of aerosol particles [2]:

$$2NaCl + O_3 \xrightarrow{H_2O} Cl_2 + 2NaOH + O_2. \qquad (A)$$

It was also found that the heterogeneous oxidation of Cl^- to Cl^0 takes place in the hydrogen chloride–ozone interaction as well [3]:

$$2HCl + O_3 \xrightarrow{H_2O} Cl_2 + H_2O + O_2. \qquad (B)$$

Since the bond in the HI molecule is much weaker than the bond in the HCl molecule, it could be assumed that the reaction between hydrogen iodide and ozone can proceed via both heterogeneous and homogeneous routes. In our study, we investigated the formation of iodine atoms in the reaction between HI and ozone, using resonance fluorescence (RF) in the detection of I atoms.

EXPERIMENTAL

Kinetic measurements were based on the RF method applied to the detection of iodine atoms. This method was also employed in an earlier study [4]. The principle of this method is as follows. The resonance radiation of atoms is directed to a reactor containing the same atoms. Reemitted photons are detected in a direction perpendicular to the direction of the resonance lamp emission. Since the resonance lines of atoms are generally in the vacuum UV region [5], the registration of photons requires special techniques, namely, windows made from an appropriate material and detectors sensitive to vacuum ultraviolet. Owing to its high sensitivity, this method enabled us to investigate processes involving low concentrations of iodine atoms and $IO^{\bullet}$ radicals and to eliminate the effect of the fast reactions between $IO^{\bullet}$ radicals [6].

Our experimental setup consisted of a flow reactor, a source of iodine atoms, an iodine atom detection system, and a reactant inlet system. This setup allowed constant reactant flow rates to be maintained with an accuracy of ~2–3% over 10–15 h.

The reactor (Fig. 1) was a quartz tube with a diameter of 1.3–1.6 cm. The gases to be reacted were delivered to the reactor through quartz inlet pipes with a diameter of 10 mm, which were connected to the reactor using quartz capillaries 1 mm in diameter and 10 mm in length. These capillaries minimized the retrodiffusion of the reactants. The reactor was equipped with a source of iodine atoms. The gas pressure in the reactor was measured with a VDG-1 manometer in the 1–10 Torr range with an accuracy of ~0.03 Torr (2%). The reactor surface was lined with F-32L fluoroplast in order to reduce the heterogeneous loss of iodine atoms (or $IO^{\bullet}$ radicals).

The source of iodine atoms was a quartz tube with a diameter of 15 mm and a length of 300 mm. This tube was soldered with a thinner tube 4 mm in diameter and 400 in length. The thinner tube, with a Teflon stocking-type seal, could be moved along the reactor axis without causing a seal failure, making it possible to vary the reactant contact time. A bactericide lamp was mounted on the thicker tube. A mixture of helium and gaseous

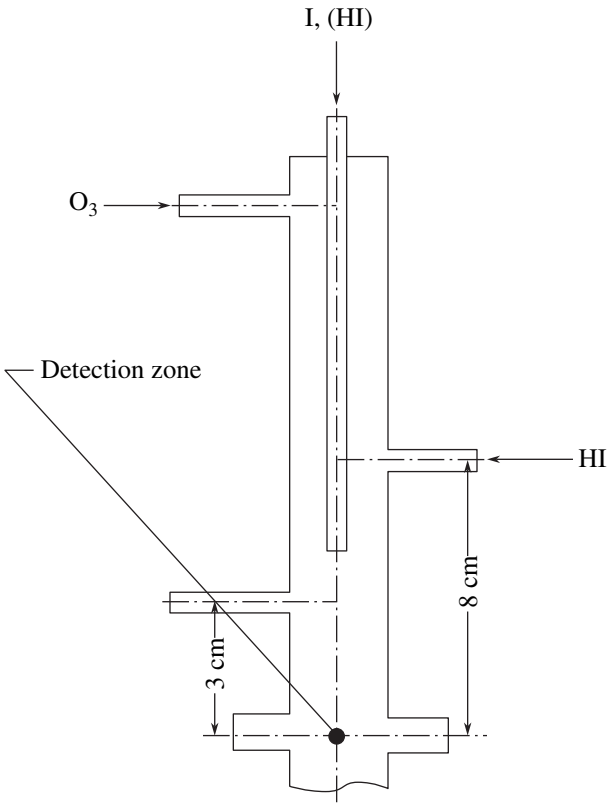

Fig. 1. Schematic of the flow reactor used in the investigation of the reaction HI + O_3.

methyl iodide was passed through the iodine atom source. Under the action of λ = 253.7 nm light, methyl iodide yielded iodine atoms in the $^2P_{1/2}$ and $^2P_{3/2}$ states (20% of the atoms were in the ground state $^2P_{3/2}$ [7]). Part of the iodine atoms were deexcited into the $^2P_{3/2}$ state in the source of atoms on CH_3I molecules, and part, in the reactor on oxygen molecules.

The iodine atom detection zone consisted of tubes ~10 mm in diameter and ~10 mm in length soldered crosswise into the reactor. The tubes ended with quartz sockets, in which the brass cones of a resonance lamp and of a photon counter and Wood horns were secured using vacuum grease. The Wood horns served to reduce the backscatter of resonance radiation. Copper tubes were fitted into the cones of the lamp and photon counter. They served both to collimate the radiation from the resonance lamp and to enhance the heterogeneous loss of the iodine atoms diffusing into the crossed tubes from the reactor.

The copper tubes and the inner surfaces of the cross were coated with MgO for a higher loss rate of iodine atoms.

The system for detecting the resonance fluorescence of iodine atoms consisted of an iodine resonance lamp, a photoionization detector, and a Ch3-63/1 frequency meter connected to a computer. This system carried out signal registration and accumulation and subsequent data processing.

The flow-type iodine resonance lamp was operated at a wavelength of λ = 178.3 nm, at which the absorption cross section for the resonance radiation of iodine atoms was the largest: $\sigma^{res}_{\lambda = 178.3\ nm}(I) = 5 \times 10^{-13}$ cm^2 [8]. The lamp was made from quartz, and the windows were made from quartz (UF brand) with a short-wavelength transmission cutoff at 160 nm. Vacuum sealing was achieved using indium gaskets. The diiodine concentration at the inlet of the resonance lamp was ~7×10^{12} molecules per cubic centimeter.

Gas discharge in the lamp was initiated with a Breid microwave resonator.

The photoionization counter detecting 160- to 185-nm radiation is described in detail in an earlier paper [4]. Signals were accumulated with a computer attached to a Ch3-63/1 frequency meter; 500 to 2000 pulses were accumulated at each experimental point. The end window of the counter was made of quartz (UF brand) with a short-wavelength transmission cutoff at ~160-nm.

The counter was pumped to 5×10^{-5} Torr using a diffusion pump and was then filled with a mixture of NO (10 Torr) and Ar (230 Torr). A drop of diethylferrocene was placed into the glass "appendix" of the counter. Diethylferrocene vapor was in equilibrium with the drop. The long-wavelength cutoff edge of the counter, determined by the ionization potential of diethylferrocene (6.3 eV [9]), was ~185 nm.

Thus, the photoionization counter served as a monochromator as well, separating the spectral range between ~160 and ~185 nm.

The absolute iodine-atom sensitivity of the setup was calibrated against the known iodine atom concentration established by adding diiodine to an excess amount of oxygen atoms. The following reactions took place in this system:

$$O + I_2 \xrightarrow{k_a} IO^{\bullet} + I, \quad (a)$$

$$k_a = 1.4 \times 10^{-10}\ \text{cm}^3\ \text{molecule}^{-1}\ \text{s}^{-1},\ [10];$$

$$O + IO^{\bullet} \xrightarrow{k_b} I + O_2, \quad (b)$$

$$k_b = 5 \times 10^{-11}\ \text{cm}^3\ \text{molecule}^{-1}\ \text{s}^{-1},\ [11];$$

$$I \xrightarrow{\text{wall}, k_c} 1/2\, I_2, \quad k_c < 10\ \text{s}^{-1}. \quad (c)$$

Oxygen atoms were produced in a microwave discharge in a 4%O_2 + He mixture. The oxygen atom concentration was estimated by chemiluminescence titration with NO_2 [12].

The steady-state concentration of diiodine and $IO^{\bullet}$ radicals in this source of iodine atoms was far below 1% of the iodine atom concentration. Indeed, the steady-state I, $IO^{\bullet}$, and I_2 concentrations established in

a time of about $1/k_b[O] = 2 \times 10^{-4}$ s were interrelated as follows:

$$[I_2] = [I]\frac{k_c}{2k_a[O]} \le [I] \times 10^{-3}\ \text{cm}^{-3}, \quad (1)$$

$$[IO^{\cdot}] = [I]\frac{k_c}{2k_b[O]} \le [I] \times 2 \times 10^{-4}\ \text{cm}^{-3}. \quad (2)$$

Therefore, nearly all of the iodine was in atomic form, so it was possible to determine the absolute iodine-atom sensitivity of the system from the dependence of the resonance fluorescence signal on the amount of diiodine introduced into the reactor.

The O concentration was almost three orders of magnitude higher than the I concentration.

In the investigation of the reactions of the $IO^{\cdot}$ radical, the iodine-atom sensitivity of the system was determined as follows. Diiodine from a calibrated tube entered the reactor, where it reacted with oxygen atoms. Oxygen atoms were produced by passing O_2 and He (1 : 6) through a microwave discharge. The volume of the calibrated tube was 220 cm^3, and the gas pressure in the reactor was 1.2 Torr. Iodine atoms resulted from reactions (a)–(c). The absolute iodine-atom sensitivity of the system appeared to be $\sim 3 \times 10^7$ cm^{-3}, the signal-to-noise ratio was equal to unity, and the pulse accumulation time was ~100 s.

All gaseous reactants but CH_3I were fed into the reactor using flow controllers, which allowed a preset gas flow rate to be maintained with an accuracy of 2–3% over 10–15 h.

The gas from a cylinder passed though a calibrated vessel with a standardized manometer, a flow controller, and a metallic diffusion valve and then entered the reactor.

The mass flow rates of the reactants and carrier gases were determined by measuring the gas outflow from the calibrated vessel per unit time.

Ozone was produced by passing O_2 through an Ozon-2 ozone generator. The oxygen + ozone mixture from the ozone generator was passed through a 10-cm-long glass cell placed in a Spectromom-204 spectrophotometer for measuring the ozone concentration. The cell had quartz windows, and its outlet was fitted with a glass–Teflon regulating valve. This valve allowed the gas pressure in the optical cell to be varied between 10 and 100 Torr without affecting the mass flow rate. This enabled us to find an absorbance range convenient for measurements. Next, the $O_2 + O_3$ mixture entered the reactor. The ozone concentration was derived from the change in absorbance at $\lambda = 253.7$ nm using the formula

$$[O_3] = \frac{Q(O_3)}{Q_\Sigma}\Sigma[C_i]. \quad (3)$$

Here, Q_Σ is the total gas flow rate in the reactor and $Q(O_3)$ is the ozone flow rate in the reactor (the amount of ozone entering the reactor in 1 s):

$$Q(O_3) = Q(O_2 + He)\frac{2.3D_{10}}{\sigma L_c P_c \times 3.25 \times 10^{16}}. \quad (4)$$

Here, $Q(O_2 + He)$ is the total gas flow rate in the ozone generator (cm^3 Torr s^{-1}), D_{10} is absorbance (on the decimal logarithmic scale), 2.3 is the decimal-to-natural logarithm conversion factor, $\sigma_{253.7\ nm} = 1.15 \times 10^{-17}$ cm^2 is the absorption cross section for ozone at $\lambda = 253.7$ nm, $L_c = 10$ cm is the cell length, P_c is the gas pressure in the cell (Torr), and $\Sigma[C_i]$ is the total concentration of species in the reactor:

$$\Sigma[C_i] = \frac{P_r \times 9.7 \times 10^{18}}{T}. \quad (5)$$

In this formula, P_r is the reactor pressure (Torr) and T is the reactor temperature (K).

The $O_2 + O_3$ stream between the cell and the reactor was in contact only with glass and Teflon surfaces, on which ozone did not decompose. The ozone concentration in the reactor was controlled by varying the ozone generator voltage at constant flow parameters.

All of the oxygen molecules in the excited states $^1\Delta_g$ and $^1\Sigma_g^+$ that formed in the ozone generator disappeared by reacting with ozone:

$$O_2(^1\Delta_g) + O_3 \longrightarrow 2O_2 + O,$$

$$k = 1.1 \times 10^{-15}\ \text{cm}^3\ \text{molecules}^{-1}\ \text{s}^{-1}\ [13];$$

$$O_2(^1\Sigma_g^+) + O_3 \longrightarrow 2O_2 + O,$$

$$k = 2.5 \times 10^{-11}\ \text{cm}^3\ \text{molecules}^{-1}\ \text{s}^{-1}\ [14].$$

This took about 1 s, the time necessary for the gas at a pressure of 760 Torr to pass through the connecting pipes before arriving at the control valve.

Diiodine was fed into the reactor as follows. A calibrated ampule with a Teflon valve and iodine crystals inside was filled with helium to a pressure of 200 Torr. The ampule was placed in a cold trap, and the trap was immersed into melting ice. The saturation vapor pressure of diiodine at the melting-ice temperature is 3.2×10^{-2} Torr [9]. The ampule was connected to the reactor through the Teflon valve.

The concentration of diiodine entering the reactor was calculated using the formula

$$[I_2] = \frac{Q_{He+I}[I_2]_{amp}}{Q_\Sigma}P_r \times 3.16 \times 10^{16}, \quad (6)$$

where Q_{He+I} is the mass rate of gas outflow from the calibrated ampule (cm^3 Torr s^{-1}), $[I_2]_{amp}$ is the diiodine fraction in the ampule, Q_Σ is the total mass flow rate in the reactor (cm^3 Torr s^{-1}), and 3.16×10^{16} cm^{-3} is the Loschmidt number for $P = 1$ Torr and $T = 298$ K.

Diiodine was entered into the resonance lamp as follows. Helium from a cylinder was passed through a liquid-nitrogen cold trap and then through a flow controller, which measured the mass flow rate as the rate of gas outflow from a calibrated vessel. The flow controller maintained the preset outlet gas pressure at a variable inlet pressure. The flow control system allowed any outlet pressure in the 10–760 Torr range to be established. Next, helium was passed through the glass vessel containing iodine crystals at room temperature and a coiled trap immersed in melting ice and was entered into the resonance lamp through a glass capillary. The iodine line was a single glass piece and had no greased joints.

Iodine atoms were obtained by the photolysis of CH_3I (0.1–1%) in O_2 at $\lambda = 253.7$ nm. CH_3I was stored as a liquid in glass bottles in the dark. During experiments, the bottles were immersed in melting ice. CH_3I vapor was introduced, using a metering valve, into oxygen flowing through the source of iodine atoms. The flow rate was determined by measuring the pressure drop in the calibrated vessel. CH_3I was reagent grade. The photolysis of CH_3I resulted in I atoms and $CH_3^{\cdot}$ radicals. The latter reacted with oxygen to form $CH_3O_2^{\cdot}$, a low-activity radical. The other processes occurring in the iodine atom source and their possible effects on the measurements were detailed in our earlier publication [4].

RESULTS AND DISCUSSION

Because we expected that the reaction between hydrogen iodide and ozone in the reactor would yield iodine atoms and $IO^{\cdot}$ radicals, we first determined the loss rate constants for these species on the surface of our reactor.

Heterogeneous Loss of Iodine Atoms and $IO^{\cdot}$ Radicals

Measurements were carried out in the reactor schematized in Fig. 1. The heterogeneous loss of atoms was investigated by measuring the resonance fluorescence of iodine atoms as a function of the distance L between the atomic iodine introduction point and the detection zone. With neglect of the axial diffusion and radial distribution, the following formula is valid for the concentration of iodine atoms:

$$[I] = [I]_0 \exp(-k_h \tau). \quad (7)$$

Hence, the rate constant of the heterogeneous process is

$$k_h = -\frac{1}{\tau} \ln [I]/[I]_0, \quad (8)$$

where $\tau = L/v$ is the time required for the atoms moving with the mass-average linear velocity v to travel the distance L.

Expression (8) was also employed to determine the rate of the heterogeneous loss of $IO^{\cdot}$ radicals. To do this, we used the following technique. Iodine atoms were fed through a nozzle into the reactor, through which ozone-containing oxygen was flowing. As was demonstrated above, the iodine atoms were almost completely converted into $IO^{\cdot}$ radicals at a distance of <1 cm from the nozzle end. At a distance of 3 cm from the detection zone, the $IO^{\cdot}$ radicals were almost completely reconverted into iodine atoms by reacting with NO. The signal from the iodine atoms was registered by the counter.

Next, ln ln$[I]/[I]_0$ was plotted versus τ and the plot was fitted to a straight line by least squares. The rate constants of the heterogeneous loss of I and $IO^{\cdot}$ were determined from the slope of this line to be 132 ± 9 and 43 ± 5 s^{-1}, respectively.

Kinetics and Mechanism of the Reaction between Hydrogen Iodide and Ozone

The experiments were carried out in the reactor shown in Fig. 1, but the source of iodine atoms was replaced with a hydrogen iodide inlet system and oxygen-diluted ozone was fed through a side inlet. Iodine atoms were detected in the reactor. The intensity of the RF signal from I atoms (J) and, accordingly, the concentration of I atoms were measured as a function of hydrogen iodide and ozone concentrations in the reactor at $T = 295$ K and $P = 2.08$ Torr. The signal intensity J was calibrated against the iodine atom concentration prior to each series of experiments. The ozone concentration in the flowing gas was controlled by varying the ozone generator voltage. This allowed the stream parameters (pressure and flow rate) to be kept constant. The relationships thus established are plotted in Fig. 2. The RF signal from iodine atoms is a linear function of the hydrogen iodide concentration throughout the measurement range (Fig. 2a). By contrast, only the initial portion of the plot shown in Fig. 2b can be fitted to a straight line: at higher ozone concentrations, there is a marked deviation from linearity.

These dependences of the iodine atom concentration on the ozone and hydrogen iodide concentrations were explained in terms of the following reaction mechanism.

The chain initiation reactions are the following:

$$HI + O_3 \xrightarrow{k_1} I + OH^{\cdot} + O_2, \ \Delta H = -29 \text{ kcal/mol}, \quad (I)$$

$$OH^{\cdot} + HI \xrightarrow{k_{1a}} I + H_2O. \quad (Ia)$$

The chain propagation reactions are

$$I + O_3 \xrightarrow{k_2} IO^{\cdot} + O_2, \quad (II)$$

$$IO^{\cdot} + HI \xrightarrow{k_3} I + HOI^{\cdot}. \quad (III)$$

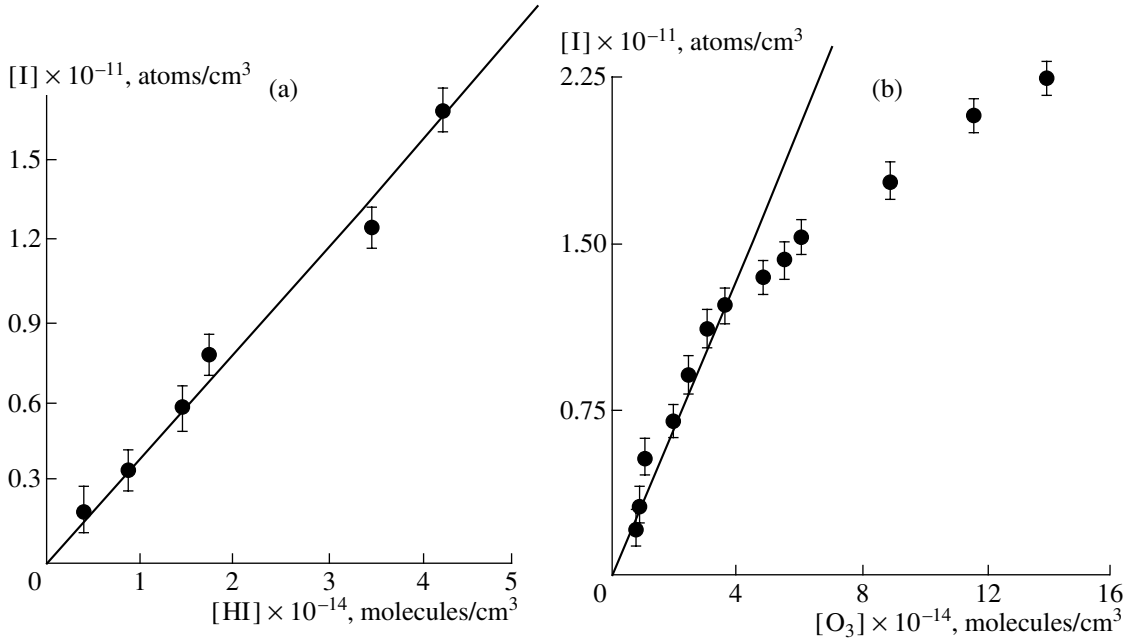

Fig. 2. Concentration of iodine atoms (a) as a function of the HI concentration at $[O_3] = 4.0 \times 10^{14}$ cm^{-3} and (b) as a function of the ozone concentration at $[HI] = 4.1 \times 10^{14}$ cm^{-3}. $T = 295$ K; $P = 2.08$ Torr.

The chain termination reactions (the loss of radicals on the walls) are represented as

$$I + \text{wall} \xrightarrow{k_4} \text{products}, \quad \text{(IV)}$$

$$IO^{\cdot} + \text{wall} \xrightarrow{k_5} \text{products}. \quad \text{(V)}$$

The variation of the concentrations of active species is described by the equations

$$\frac{\partial[OH^{\cdot}]}{\partial t} = k_1[HI][O_3] - k_{1a}[OH^{\cdot}][HI], \quad (9)$$

$$\frac{\partial[IO^{\cdot}]}{\partial t} = k_2[I][O_3] - k_3[IO^{\cdot}][HI] - k_5[IO^{\cdot}], \quad (10)$$

$$\frac{\partial[I]}{\partial t} = k_1[HI][O_3] + k_{1a}[OH^{\cdot}][HI] - k_2[I][O_3] + k_3[IO^{\cdot}][HI] - k_4[I]. \quad (11)$$

Under steady-state conditions,

$$[I] = \frac{2k_1[HI][O_3]}{k_2[O_3]\left(1 - \frac{k_3[HI]}{k_3[HI] - k_5}\right) + k_4}. \quad (12)$$

Setting

$$[I]_1 = \frac{2k_1[HI][O_3]}{k_4}, \quad (13)$$

we obtain

$$\frac{[I]_1}{[I]} = \frac{k_2[O_3](1 - X)}{k_4} + 1, \quad (14)$$

where

$$X = \frac{k_3[HI]}{k_3[HI] + k_5}. \quad (15)$$

It follows from Eq. (12) that, at low ozone concentrations and not very low HI concentrations, the iodine concentration and, hence, the RF signal vary linearly with the ozone concentration. Furthermore, Eq. (12) predicts that raising the ozone concentration, implying an increase in the first term of the denominator of Eq. (12), will cause nonlinearity. This prediction is in agreement with the plot shown in Fig. 2b.

From the slope of the initial, linear portion of the [I] versus $[O_3]$ plot and the earlier determined k_4 value, we found that the rate constant of reaction (I) is

$$k_1 = (5.25 \pm 1.5) \times 10^{-17} \text{ cm}^3/\text{s}.$$

As determined from the plot of the RF signal from iodine atoms versus the hydrogen iodide concentration (Fig. 2a), the rate constant is equal to

$$k_1 = (5.65 \pm 1.80) \times 10^{-17} \text{ cm}^3/\text{s}.$$

The mean rate constant of reaction (I) derived from the two series of experiments is

$$k_1 = (5.45 \pm 1.80) \times 10^{-17} \text{ cm}^3/\text{s}.$$

Even though reaction (I) is exothermic and proceeds without any steric hindrance, its rate constant seems to be too large for a reaction between saturated com-

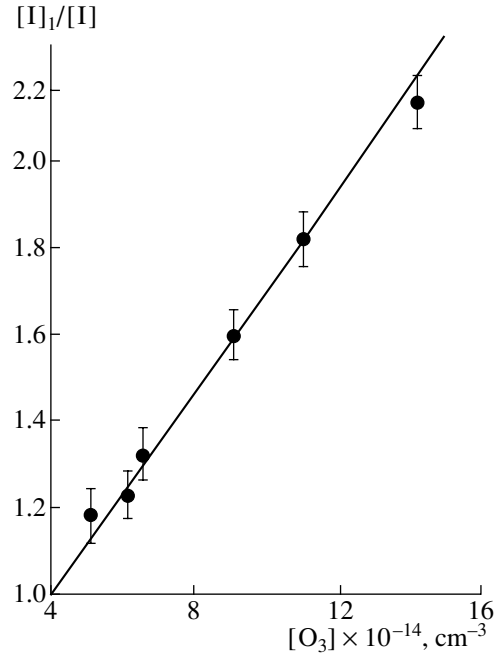

Fig. 3. $[I]_1/[I]$ as a function of the ozone concentration. T = 295 K; P = 2.08 Torr; [HI] = 4.1×10^{14} cm^{-3}.

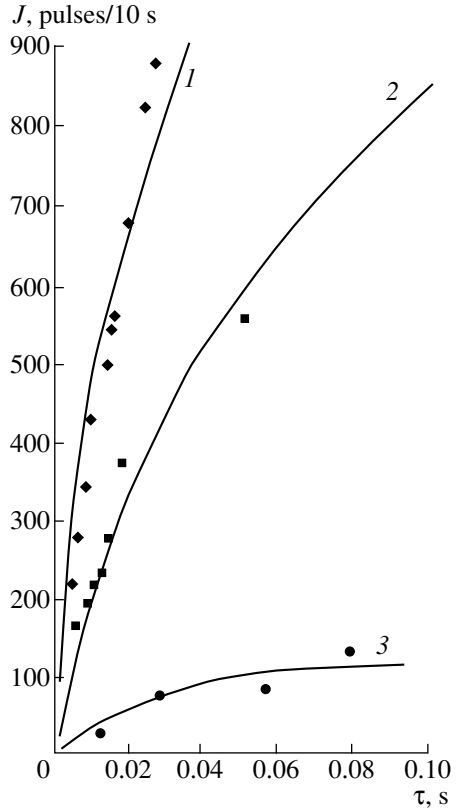

Fig. 4. Intensity of the RF signal from iodine atoms versus the HI–O_3 contact time. The points represent experimental data; the curves represent data calculated for (*1*) [HI] = 4.5×10^{14} cm^{-3} and [O_3] = 1.55×10^{15} cm^{-3}, (*2*) [HI] = 2.8×10^{14} cm^{-3} and [O_3] = 1.55×10^{15} cm^{-3}, and (*3*) [HI] = 1.8×10^{14} cm^{-3} and [O_3] = 2.3×10^{14} cm^{-3}.

pounds. It is possible that this reaction, like reactions (A) and (B), occurs in part on the surface. We demonstrated in an earlier study [15] that some reactions involving iodine-containing species are heterogeneous despite the fact that their rates show the same dependence on the reactant concentrations as the corresponding homogeneous reaction. Apparently, the discrepancy between rate constant data reported by different researchers for the same reaction (which is sometimes as large as one order of magnitude or even greater) is due to difficulties in distinguishing between the homogeneous and heterogeneous mechanisms of the reaction.

Figure 3 plots $[I]_1/[I]$ versus $[O_3]$. The $[I]_1$ value was determined by extrapolating the linear portion of the curve shown in Fig. 2b to high ozone concentrations. Knowing the k_4 and k_5 values (determined earlier) and the rate constant k_2 [16], we derived, from the slope of the straight line in Fig. 3, the chain-propagation rate constant k_3:

$$k_3 = (1.1 \pm 0.4) \times 10^{-12} \text{ cm}^3/\text{s}.$$

In order to validate the above reaction mechanism and make sure that the rate constants of the reactions involved in this mechanism were measured accurately, we carried out a numerical simulation of the process and compared the results with experimental data. The following series of experiments was performed. A certain concentration of HI was introduced into flowing diluted ozone through a movable nozzle. The nozzle was moved along the reactor axis, and the signal intensity J and, accordingly, the concentration of iodine atoms were measured as a function of the reaction time at various HI and ozone concentrations. Next, theoretical curves describing the time variation of the iodine concentration were plotted for the above reaction mechanism. The necessary rate constants were either known from earlier experiments or taken from the literature [16, 17]. The experimental data points were plotted together with the theoretical curves (Fig. 4). The experimental and theoretical data are in good agreement. This is evidence that the mechanism suggested here is valid and that the rate constants of the reactions involved in this mechanism are determined with a rather high degree of accuracy.

REFERENCES

1. Sturges, W.T. and Barrie, I., *Atmos. Environ.*, 1988, vol. 22, p. 1101.
2. Keene, W.C., Pszenny, A.P., Jacob, D.J., Duce, R.A., et al., *Global Biogeochem. Cycles*, 1990, vol. 4, no. 4, p. 407.
3. Behnke, W. and Zetsch, C., *J. Aerosol Sci.*, 1989, vol. 20, no. 8, p. 1167.
4. Buben, S.N., Larin, I.K., Messineva, N.A., and Trofimova, E.M., *Khim. Fiz.*, 1989, vol. 8, no. 9, p. 1234.
5. Clyne, M.A.A. and Townsend, L.W., *J. Chem. Soc., Faraday Trans. 2*, 1974, vol. 70, no. 9, p. 1863.

6. Jenkin, M.E. and Cox, R.A., *J. Phys. Chem.*, 1985, vol. 89, p. 192.
7. Okabe, H., *Photochemistry of Small Molecules*, New York: Wiley, 1978.
8. Mitchel, A. and Zamansky, M., *Resonance Radiation and Excited Atoms*, Cambridge: Cambridge Univ. Press, 1934.
9. Kikoin, I.K., *Tablitsy fizicheskikh velichin* (Physical Data in Tables), Moscow: Atomizdat, 1976.
10. Ray, C.W. and Watson, R.J., *J. Phys. Chem.*, 1981, vol. 85, no. 20, p. 2955.
11. Baulch, D.O., Cox, R.A., and Hampson, R.J., Jr., et al., *CODATA*, 1982, no. 6, p. 982.
12. *Fizicheskaya khimiya bystrykh reaktsii* (Physical Chemistry of Fast Reactions), Zaslonko, I.S., Ed., Moscow: Mir, 1976, p. 306.
13. Collins, R.J., Hussain, D., and Donovan, R.J., *J. Chem. Soc., Faraday Trans. 2*, 1973, vol. 69, no. 1, p. 145.
14. Filseth, S.V., Zia, A., and Welg, K.H., *J. Chem. Phys.*, 1970, vol. 52, no. 1, p. 5502.
15. Buben, S.N., Larin, I.K., Spasskii, A.I., Trofimova, E.M., and Turkin, L.E., *Khim. Fiz.*, 2002, vol. 21, no. 4, p. 59.
16. Buben, S.N., Larin, I.K., Messineva, N.A., and Trofimova, E.M., *Khim. Fiz.*, 1990, vol. 9, no. 1, p. 116.
17. Orkin, V.L. and Khamaganov, V.G., *J. Atmos. Chem.*, 1993, vol. 16, no. 2, p. 157.